Gigaton Commercial-Scale Carbon Storage and Mineralization Potential in Stacked Columbia River Basalt Reservoirs

Ruoshi Cao [a]*, Quin R.S. Miller [a]*, Casie L. Davidson [a], William Gallin [b], Stephen P. Reidel [a#], Zunsheng Jiao [c], J. Fred McLaughlin [c], Emily T. Nienhuis [d], H. Todd Schaef [a]

[a] Earth and Environment Directorate, Pacific Northwest National Laboratory, Richland, WA, 99354, USA

[b] Washington Department of Natural Resources, Washington Geological Survey, Olympia, WA, 98504, USA

[c] Center for Economic Geology Research, University of Wyoming, 1000 E. University Avenue, Laramie, WY, 82071, USA

[d] Physical and Computational Sciences Directorate, Pacific Northwest National Laboratory, Richland, WA, 99354, USA

[#] Retired

KEYWORDS: geologic carbon sequestration; supercritical carbon dioxide; basalts; mineralization; anticline; storage resources; stacked reservoirs

ABSTRACT**:** This work presents a detailed supercritical CO_2 storage resource estimation for the stacked basalt reservoirs in the Grande Ronde Basalt of the Columbia River Basalt Group in eastern Washington and Oregon. The assessment aims to derisk the commercialization potential of geologic carbon storage in basalt by leveraging physical and mineralization trapping of CO_2 in basalt. The structural closures formed by anticlinal ridges and synclinal valleys in Yakima Fold Belt are excellent physical traps to accommodate injected supercritical CO_2. Rigorous hydraulic testing, well logs and simulation results from the Wallula Basalt Pilot #1 well showed the occurrence of 17 suitable permeable injection zones (up to 2,496 mD) intercalated with dense seals (~2.6E-10 mD) in the Grand Ronde Basalt. In addition, geochemical studies showed fast reactions between supercritical CO_2 and dissolved basalt minerals to form stable carbonates. Our calculation indicates up to 40 gigatons (P90) of mineralization storage resources exist in the Grande Ronde Basalt reservoirs.

1. Introduction

Columbia River Basalt Group (CRBG) extends over a large area and is coincident with a very large fraction of the power generation and industrial CO_2 sources in the Pacific Northwest (PNW). However, because flood basalts represent a significant barrier for oil and gas exploration in the underlying sedimentary rock, this region is sparsely investigated relative to conventional

sedimentary basins. Only very limited data are available on deep reservoir hydrogeologic properties that are critical to any quantitative assessment of potential for CO_2 storage.

To address these data gaps, Pacific Northwest National Laboratory (PNNL) has pioneered both laboratory (McGrail et al., 2009a; McGrail et al., 2006; Schaef et al., 2014; Schaef and McGrail, 2009; Schaef et al., 2010; Schaef et al., 2011; Xiong et al., 2018) and field pilot studies (Depp et al., 2022; McGrail et al., 2017; McGrail et al., 2009c; Polites et al., 2022; White et al., 2020) examining the potential for large-scale injection and storage of CO_2 and natural gas (Reidel et al., 2002) in flood basalts. The PNNL-led Wallula Basalt Carbon Storage Pilot Project demonstrated the successful injection and mineralization of 977 tons of supercritical CO_2 ($scCO_2$) in the interflow zones of the Grand Ronde Basalt (GRB) near the town of Wallula in eastern Washington State. The post-injection core samples and hydrologic simulation reported that up to 60% of injected CO_2 had been incorporated into carbonate minerals within two years of injection (White et al., 2020). The simulated mineralization rate was consistent with laboratory observation, thus offering a highly secure pathway to permanent geologic CO_2 storage.

With an expansion of the 45Q tax credit in 2022, the PNW has an unprecedented opportunity to leverage a groundswell of interest and enthusiasm from potential industry partners. Based on the pilot-scale field tests, simulation modeling, and geochemical analysis, this paper provides a robust CO_2 pore space storage resource estimation for anticlinal basalt reservoirs. The storage resource estimation laid the foundation for future deployment of commercial-scale carbon capture (such as point source or direct air capture (DAC)) at favorable locations in the PNW and characterization approaches necessary to support successful application for the U.S. Environmental Protection Agency Class VI wells used for geologic sequestration of CO_2 (Class VI wells) for the basalt reservoir class (**Figure 1**).

To meet the safety and effectiveness criteria as potential storage sites (Bachu, 2007), the basalt storage system should have 1) sufficient pressure and temperature to maintain CO_2 in supercritical state, 2) confinement units to prevent vertical migration and leakage of CO_2, 3) hydrogeologic conditions that isolate CO_2 from underground sources of drinking water aquifers, and 4) good injection rate for commercial-scale CO_2 sequestration. Hydrological modeling and petrophysical log analysis suggested suitable conditions exist at depths deeper than 750 m below ground surface (bgs) in the Yakima Fold Belt. Stratigraphically, these favorable reservoir conditions occur in the GRB of the CRBG (Reidel et al., 2003; Reidel et al., 1989) (**Figure S1**). The unique structure of the basalt flows produced alternating permeable interflow zones and dense flow interiors stacked below any individual storage site (Gierzynski and Pollyea, 2017; McGrail et al., 2006) (**Figure S2**).

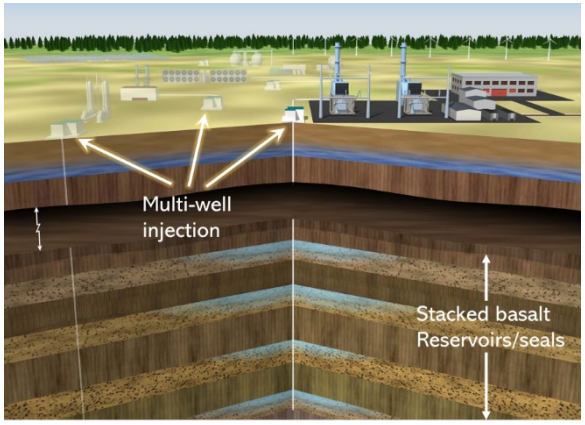

Figure 1. Conceptual illustration of deep (>750 m below ground surface) stacked Columbia River Basalt reservoirs in the Pacific Northwest that can accommodate commercial-scale carbon capture and storage hubs.

Although the potential of CO_2 storage in basalt reservoirs has been studied at several sites around the world, there has been no standardized methodology to estimate the storage resource. We compare the methodologies used to calculate the CO_2 storage load (kg/m^3) in three types of basalt reservoirs. For the continental flood basalt, the CRBG was estimated to be able to store more than 100 gigatons of CO_2 in an area of about 146,000 km^2 (McGrail et al., 2006). McGrail et al. volumetrically calculated the free-phase CO_2 storage potential in pore space, assuming an interflow thickness of 10 m, 10 interflow zones, average porosity of 15%, and at about 1,000 m below ground. This results in 40.65 kg of CO_2 load per cubic meter of basalt reservoir. (Vishal et al., 2021) applied the same method and estimated the total CO_2 storage capacity in Deccan Volcanic Province and Rajmahal Traps to be 316 Gt. For the mid-ocean ridge basalts in the Juan de Fuca plate, (Goldberg et al., 2008) used the pore-filling method and estimated that 7,800 km^3 of deep-sea basalt reservoir can store about 926 Gt of CO_2 if all of the CO_2 becomes fixed carbonate. Goldberg et al. assumed a channel system dominates the permeability over one-sixth of the upper 600 m of basement, and the average channel porosity is 10%. This results in a CO_2 storage load of 119 kg/m^3. For the mid-ocean ridge basalt in Iceland, (Snæbjörnsdóttir et al., 2014) developed their natural analogues method based on a study done by (Weise et al., 2008) where the amount of calcite was measured in well cuttings from three geothermal systems. The geothermal systems in Iceland receive considerable amounts of CO_2 from magma chambers or intrusions at the roots of the systems and is considered as a natural experiment to determine the CO_2 storage capacity of the basalt. The average CO_2 load in Iceland basalt is calculated to range from 18.8 to 48.7 kg/m^3. For the ocean island basalt, (Li et al., 2023) applied total mineralization method and estimated 257 km^3 of Leizhou Peninsula basalt can store 30.8 – 45.9 Gt of CO_2. Li's method assumes all CaO, MgO, and FeO in the basalt will fully react with CO_2 to form carbonates and results in 119 – 179 kg/m^3 of CO_2 load in the basalt. Furthermore, (Stanfield et al., 2024) applied a more realistic mineralization assessment to calculate the storage potential in the olivine-rich Hawai'i basalt. The method uses the reactive volume fraction that is derived from pore surface area, reaction depth, and volume of basalt to represent the portion of the basalt that can react with CO_2. The result shows that the olivine-rich Hawai'i basalt can

Table 1. Comparison of in situ carbon storage potential assessment methods in different basalt types

Basalt type	Location	Porosity	Storage load[d] (kg/m^3)	Capacity (Gt)	Methods	References
CFB[a]	Columbia River Basalt (US)	15%	40.65	100	Pore space volumetrics	(McGrail et al., 2006)
CFB	DVP[b] and Rajmahal Traps (India)	15%	40.65	315.85	Pore space volumetrics	(Vishal et al., 2021)
MORB[a]	Juan de Fuca plate(offshore US)	10%	119	926	Pore-filling	(Goldberg et al., 2008)
MORB	Iceland	10-15%	18.8-48.7	953-2,470	Natural analogues	(Snæbjörnsdóttir et al., 2014)
OIB[a]	Leizhou Peninsula (China)	8.9%	119-179	30.8-45.9	Total mineralization	(Li et al., 2023)
OIB	Hawai'i olivine-rich basalt	25.5%	2.2	>50 MMT[c]	Partial mineralization	(Stanfield et al., 2024)

[a] CFB = Continental flood basalt, MORB = Mid-ocean ridge basalt, OIB = Ocean island basalt.

[b] DVP = Deccan Volcanic Province.

[c] MMT = Million metric ton.

[d] Storage load = Amount of CO_2 can be stored per cubic meter of basalt reservoir.

provide 2.2 kg/m^3 of CO_2 storage load. The summary of the storage assessment methods are provided in **Table 1**.

Under the Bipartisan Infrastructure Law, the US Department of Energy (DOE) defined the large-scale CCS operations as storage complexes having sufficient capacity to store minimum of 50 million metric tons (MMT) of CO_2 - the equivalent to the emissions from roughly 10 million gasoline-powered cars a year. Given that no standardized storage estimation methods has been established for basalt reservoirs, we herein adopted the U.S. DOE methods (Goodman et al., 2016; Sanguinito et al., 2022) to investigate the gigaton-scale storage potential in the GRB.

2. Geologic Setting

The Miocene Columbia River Basalt Group (CRBG) consists of a thick sequence of about 300 continental tholeiitic flood-basalt flows divided into four formations in the study area – Imnaha, Grande Ronde, Wanapum, and Saddle Mountains (Swanson et al., 1979) (**Figure S1**). The flood basalt province covers over 200,000 km^2 of the PNW and have an estimated volume of more than 220,500 km^3 (Camp et al., 2003). The GRB represents the most voluminous (72%) formation in the CRBG that produced 150,400 km^3 of basalt and covered about 169,600 km^2 of the PNW in Washington, Oregon, and Idaho (Reidel and Tolan, 2013).

The northern part of the CRBG is in a broad structural basin, the Columbia Basin, lying between the Cascade Range to the west and the Idaho batholith to the east and covering more than 150,000 km^2. Concurrent with the eruption of CRBG basalt, folding and faulting in the western part of the Columbia Basin developed the generally east-west trending anticlinal ridges and synclinal valleys, collectively known as the Yakima Fold

Belt (YFB). The static trapping in these anticlinal structures accommodates the injected $scCO_2$ in permeable interflow zones (reservoirs), which are confined between dense basalt flow interiors (seals). At places where there are no large structural or stratigraphic closures, the hydrodynamic trapping assures enough time for the carbon mineralization process to complete (Bradshaw et al., 2007; IPCC, 2005).

The GRB flows typically consist of flow tops, flow interiors, and flow bottoms (**Figure S2**). Flow top is chilled, glassy, vesicular to rubbly upper crust of a flow that typically comprises ~10% of the total flow thickness; it can be as thin as a few centimeters or occupy almost the entire flow thickness (Reidel et al., 2013; Reidel et al., 2002). The flow bottom is the basal part of a lava flow and consists of glassy, chilled basalt that may be vesicular. As basalt flows encountered bodies of water or saturated sediments, the flow bottom may produce pillow-palagonite complexes, hyaloclastite complexes, foreset bedded breccias, peperites, or spiracles features (Reidel et al., 2002). The collective contact boundary section between two individual flows is referred to as the interflow zone. The flow interior may include massive basalt and/or multiple layers of colonnades and entablatures. Basalt interflow zones are the primary reservoirs in the region, and dense flow interiors commonly act as aquitards.

No structural elements negatively impact the confining system of our study area. Regionally, located in the southeastern Yakima Fold Belt, the Area of Interest consists of a broad westward-plunging (~2°) syncline between two large anticlines – the northeast trending Blue Mountains to the south and Horse Heaven Hills Anticline to the north. This broad syncline is crossed by several smaller N-S trending structures including the Reith anticline, Agency anticline, and Service anticline (Hogenson, 1964). Although the amount of closure created by the anticlines remains to be investigated, the nearby Columbia Hills anticline provides up to 152 m of closure. The eastern limb of this anticline dips more steeply (~12°) than the western limb (~6°). The attitude of the successive basalt flows in any given section are remarkably concordant, suggesting the compressional deformation postdates the extrusion of the basalt (**Figure S3**). Because of the structural trap and small radius of the CO_2 plume, fluid migration is expected to be confined within the hinge zone of the anticline.

Additionally, no known fault exists within 5-km radius of the anticlines south of the Columbia River, except for the southern part of the Service Anticline. A 6.5 km north-south trending three-component 2-D surface seismic swath profile was acquired near the Wallula Basalt Pilot #1 well. The Wallula seismic profile intersects the Olympic-Wallowa lineament (**Figure S4**), which is a major NW-SE topographic feature in Washington and Oregon that crosscuts the Columbia Basin. The Olympic-Wallowa lineament (OWL) is an alignment of geologic structures extending nearly 650 km across the PNW

(Reidel et al., 2020). Within the Columbia Basin, the OWL is a wide zone that aligns with >250 km of folds and faults that are part of the Yakima Fold Belt. An integrated interpretation of resistivity-based image logs, XRF stratigraphy and seismic data from Wallula showed a thick succession of basalt layers undisturbed by large scale faulting (Sullivan et al., 2011). Similarly, 100 Circles #1 is located on the hinge zone of Columbia Hills anticline. A fault zone occurs at 457 m in the Wanapum Basalt Formation, indicated by the encounter of repeated geologic section. The subsurface geologic conditions, hydrologic test response characteristics, vertical hydraulic head depth profile, and hydrochemical information comparisons from 100 Circles #1 well all suggest there is vertical isolation between the basalt interflow systems. These data suggest the area has robust sealing units, with total confinement capacities that greatly exceed the storage requirement.

The conditions noted above are favorable for impermeable flow interior to confine subsurface CO_2 storage. Interpretation of the preliminary structural and stratigraphic data also suggest the possibility for sufficient closure within the anticlinal structures. The confirmation of areal closure, however, is needed with additional drilling, and both vertical and areal seismic profiling.

Fluid samples from GRB contained constituents that exceeded water quality standards. Hydrochemical data from 100 Circle #1 well showed the GRB reservoirs are vertically isolated from the overlying Underground Sources of Drinking Water (USDW) (Reidel et al., 2005). The low specific conductance, low fluoride, and low chloride concentrations in the water samples from the overlying Wanapum Basalt (480-525 m below ground) was in sharp contrast to the high concentrations for the GRB water samples (618-1,067 m). Additionally, pre-injection Wallula GRB interflow zones fluid samples (832-868 m) showed increasing fluoride concentrations (3.2-11.9 mg/L) versus test zone depth. The extended cyclical pumping cycle determined a uniform fluoride concentration level of 4.98 mg/L, which exceeds both the secondary and primary drinking water standards of 2.0 and 4.0 mg/L, respectively (McGrail et al., 2014). The total dissolved solids measured for the pre-injection fluid ranged between 149-170 mg/L (McGrail et al., 2017). Other groundwater hydrochemical data in the central Columbia Basin showed iron concentrations are frequently at or above the Washington water quality standard (<300 µg/L), with some up to 6,300 µg/L. Manganese also exceeds the state safety standards (<50 µg/L) but less frequently (Reidel et al., 2002).

3. Methods

In our analysis, we considered several methodologies used globally for storage capacity in basalt (**Table 1**). The pore-filling method (Goldberg et al., 2008) and the pore space volumetrics method (McGrail et al., 2006) both assumed the entire pore space can be occupied by pure-phase CO_2 and produced over-estimated storage capacity. The effective porosity or irreducible water saturation were not taken into consideration which would decrease the maximum CO_2 saturation in the pore space. The natural analogue method (Snæbjörnsdóttir et al., 2014) has several limitations when applied to the CRBG. Firstly, the GRB reservoirs in Columbia Basin has a much lower geothermal gradient and hydrothermal circulation environment compared to Iceland which leads to different hydrochemical conditions for carbonation reactions. Secondly, the natural analogue method may not be representative for deeper reservoirs. In the uppermost 500 to 1,000 m of the Iceland geothermal systems the CO_2 content is commonly of the order of 100 kg/m^3 but it decreases sharply below that depth and nearly no CO_2 is present below 1,500 m (Weise et al., 2008). Comparably, the target depth of the GRB reservoir ranges from 800 to over 3,000 m. Thirdly, possible cement contamination in the drill cuttings may compromise the validity of drill chip samples representing the rock (Weise et al., 2008). The total mineralization method (Li et al., 2023) overestimates the

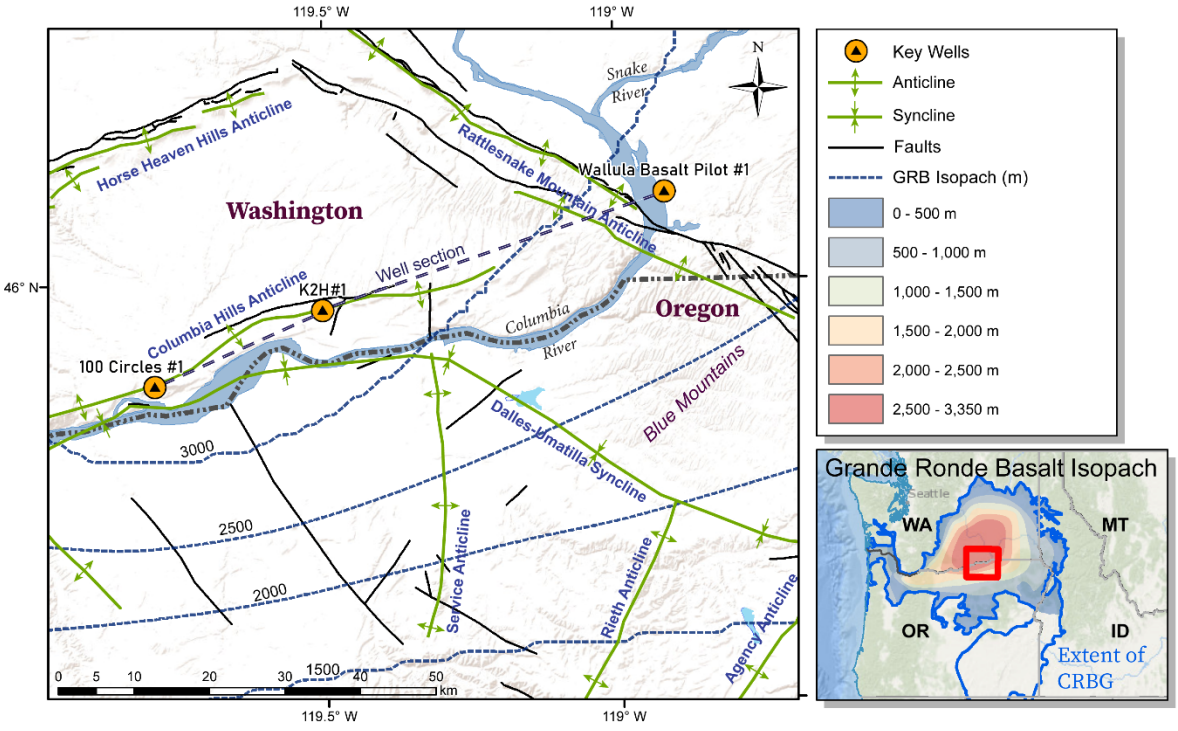

Figure 2. Structural map for the study area showing the anticlinal structures (Arlington Anticline is an informal name for the structure), faults, Grand Ronde basalt isochore thicknesses contour lines, and three correlated key deep boreholes (100 Circles #1, K2H #1, and Wallula Basalt Pilot #1).

carbon mineralization extent as the basalt is unlikely to be fully dissolved. The partial mineralization method (Stanfield et al., 2024) can more accurately estimate the mineralization extent but requires additional experimental data on the mineralogy, reaction extent, and reservoir conditions to the specific sites, and thus is not suitable for a sub-basinal scale evolution.

To estimate the free-phase CO_2 storage resource in the GRB, we adopted the US DOE method (Goodman et al., 2016; Sanguinito et al., 2022) to calculate the prospective pore space CO_2 storage resources for the basalt reservoirs (**Table 2**). This method is optimal in regions where comprehensive data are absent and excludes aquifers that are shallower than ~800 m to avoid contamination of USDW. The DOE method is a volumetric approach which calculates a mass of stored CO_2 (G_{CO2}) based on investigational area (A_t), formation thickness (h_g), porosity (Φ_{Total}), and CO_2 density (ρ) with the application of storage coefficients (E) shown in **Eq. (1)**.

$$G_{CO2} = A_t\, h_g\, \Phi_{Total}\, \rho\, E_{An/At}\, E_{hn/hg}\, E_{\Phi e/\Phi tot} E_V\, E_d \qquad \textbf{(1)}$$

The DOE efficiency factor considers a series of variables that may limit the ability of injected CO_2 to occupy 100% of the pore space, including geologic heterogeneity, gravity, or buoyancy effects, and sweep efficiency. The DOE method was designed for resource estimations in sedimentary basins, as the quantiles (P10, P50, and P90) of efficiency factors were estimated for clastics, dolomites, and limestone lithologies. Although no previous study has reported storage coefficients for basaltic reservoirs, most hydraulic testing in the CRBG suggested that the basalt interflow zones diagnostically (pressure derivative analysis) "behave" like sedimentary porous media equivalents, such as sandstones (Strait and Mercer, 1987), we adopted the site-specific storage coefficients for anticlinal sandstone reservoir with alluvial fan depositional environment from the Averaged Global Database (IEAGHG, 2009) as the best approximation for the basalt reservoir storage coefficients (**Table 2**). The volumetric results (G_{CO2}) are calculated for high, medium, and low confidence intervals of storage resource potential; P10, P50, and P90, respectively. This work followed the Goodman et al., 2016 and IEAGHG, 2009 convention, in which P10 corresponds to the smaller value that has the most certainty.

The study area (A_t = 10,000 km^2) is located in southern Columbia Basin with three key deep boreholes in the region, as shown in **Figure 2.** The thickness of the Grande Ronde Basalt (GRB) storage complex in the study area ranges from 1,500 - 3,250 m and is characterized as dozens of stacked basalt flows. There are 19 GRB members that consist of at least 90 basalt flows present in the study area (**Figure S1**). Individual flow thickness ranges from a few meters to more than 100 m, but they typically average about 30 m (Reidel and Tolan, 2013). The GRB members share relatively homogeneous bulk lithology and composition, but vary dramatically in extent and volume (Reidel and Tolan, 2013). We discuss

the properties of each five members encountered in the key wells in shown in **Figure 3**.

We integrated subsurface data from the three key wells to investigate the reservoir and seal properties of the GRB (**Figure 2**). Wallula Basalt Pilot #1, drilled in 2009, is the world's first and only successful demonstration of the injection of supercritical CO_2 into basalt interflow zones; 100 Circles #1, drilled in 1999, was a reservoir characterization well that suggested favorable conditions for natural gas storage in basalt (Reidel et al., 2005); and K2H #1 was a hydrocarbon well drilled in 1999 with limited data available. Both Wallula Basalt Pilot #1 and 100 Circles #1 have demonstrated the flow interior caprocks are capable confining units for the basalt storage system (McGrail et al., 2009b; Reidel et al., 2005; Sullivan et al., 2011). The petrophysical logs for the three boreholes used in our resource estimate are summarized in **Table S1** and were used to identify the basalt flows and characterize storage potential in the GRB.

We calculated the $scCO_2$ density variation and average formation-scale $scCO_2$ density using pressure and temperature measurements from the Wallula Basalt Polit #1 borehole and the equation of state (Span and Wagner, 1996) (implemented in NIST REFPROP, DLL version number 10.0). Additionally, we used the density to determine the total mass of CO_2 in the stacked cylindrical reservoirs as a function of variable radius. Iterative radius adjustments were made until 50 MMT of CO_2 was achieved.

Furthermore, we calculated the Area of Review (AOR) for the critical pressure and delta pressure resulted from a 30-year injection. We adopted the EPA guidance on the determination of AOR by critical pressure/pressure front (EPA, 2013). The pressure front corresponds to the minimal pressure increase needed to move fluids from the reservoir into a USDW through a hypothetical open conduit, such as an uncemented borehole or fault. The delineation of an AOR for the injection of 50 MMT CO_2 is calculated from the pressure front that derived from the results of the CO_2 injection simulations.

The critical pressure/pressure front (***Pc***) can be determine using **Eq. (2)**:

$$Pc = Pu + \rho i \cdot g \cdot (zu - zi) - Pi \qquad \textbf{(2)}$$

where:

Pu = the initial pressure at the base of the USDW (Pa=kg/m·s^2),

ρi = the density of the injection zone fluid (kg/m^3),

Table 2. CO_2 storage resource estimation (in million metric tons) in the GRB interflow zones (800 m ~ 3,000 m bgs). The DOE method's site-specific storage coefficients E is broken into five multiplicative terms ($E_{An/At}$, $E_{hn/hg}$, $E_{\Phi e/\Phi tot}$, E_V, and E_d). The $E_{An/At}$, $E_{hn/hg}$, $E_{\Phi e/\Phi tot}$ terms were based on well data and the E_V, and E_d terms were approximated from anticlinal sandstone reservoir deposited in alluvial fan environment (IEAGHG, 2009).

Parameters	P10	P50	P90	Unit	Description
A_t	10,000	10,000	10,000	km^2	Geographical area being assessed for CO_2 storage.
h_g	2,200	2,200	2,200	m	Gross thickness of saline formations for which CO_2 storage is assessed within the region defined by A_t.
Φ_{Total}	0.253	0.253	0.253	n/a	Total porosity in volume defined by the net thickness.
ρ	644	644	644	kg/m^3	Density of CO_2 evaluated at pressure and temperature that represents storage conditions anticipated for a specific geologic unit averaged over h_g and A_t.
$E_{An/At}$	0.2	0.2	0.2	n/a	Fraction of total basin or region area with a suitable formation.
$E_{hn/hg}$	0.27	0.27	0.27	n/a	Fraction of total geologic unit that meets minimum porosity and permeability
$E_{\Phi e/\Phi tot}$	0.82	0.76	0.7	n/a	Fraction of total porosity that is effective, i.e., interconnected.
E_V	0.35	0.46	0.41	n/a	Combined fraction of immediate volume surrounding an injection well that can be contacted by CO_2 and fraction of net thickness that is contacted by CO_2 as a consequence of the density difference between CO_2 and in situ water.
E_d	0.72	0.51	0.37	n/a	Fraction of pore space unavailable due to immobile in situ fluids.
E	0.0112	0.0096	0.0057	n/a	DOE storage efficiency factor.
G_{CO2}	39,998	34,512	20,554	MMT	Mass estimate (million metric tons; MMT) of saline formation CO_2 storage resource.

g = the acceleration of gravity (m/s^2),

zu = the elevation of the base of the lowermost USDW (m),

zi = the elevation of to the top of the injection zone (m), and

Pi = the initial pressure in the injection zone (Pa).

In the study area, the initial pressure at the base of the USDW is 6.895 kPa (assuming a typical 9.795 kPa/m gradient) at an elevation of 39.6 m. The pressure of the storage reservoir is 7.259 MPa at an elevation of -625.4 m above mean sea level. The density of reservoir water is 1,030 kg/m^3.

4. Results and discussion

4.1 Stratigraphy and stacked reservoir characteristics

The Wallula Basalt Pilot #1 well encountered GRB at 524 m below ground. Considering the average thickness of GRB in the study area to be about 2,500 m (**Figure 2**),

and the suitable GRB reservoir is at about 800-3,000 m bgs – the average gross thickness (h_g) of the GRB is about 2,200 m. With a net-to-gross ratio of 27%, the average net effective reservoir in GRB is about 594 m in the study area.

The Wallula Basalt Pilot #1 petrophysical logs suggested total of 17 interflow zones in Winter Water Member (WWM), Indian Ridge Member (IRM), Ortley Member (OM), Grouse Creek Member, and Wapshilla Ridge Member (**Figure 3**). These porous interflow zones are intercalated with dense flow interiors at sufficient depths (800-1,250 m below ground) capable of storing CO_2 in supercritical state.

The Winter Water Member is about 90 m thick and situated 707 m (Wallula) to 842 m (100 Circles #1) below ground. WWM consists of at least four basalt flows that are commonly glassy to fine grained and sparsely to abundantly plagioclase-phyric (Reidel and Tolan, 2013). The porosity of the interflow zones ranges from 19.5% to 30% with a net thickness of 21.6 m at 100 Circles #1 well (C4 – C7).

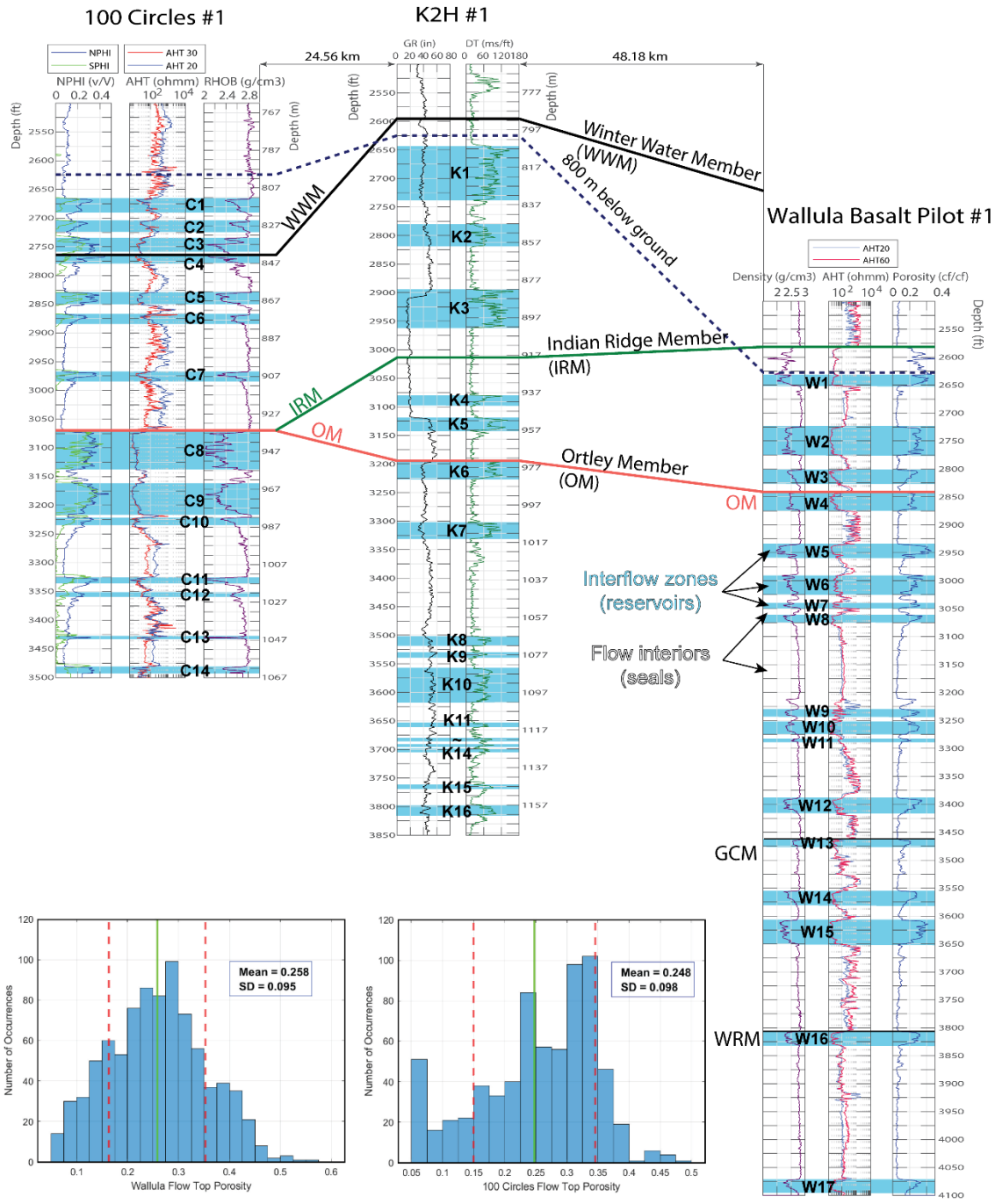

Figure 3. Well correlation between the three key wells used to characterize study area potential for commercial CO_2 storage. Each flow member consists of interflow zones (reservoirs, C1–C14, K1–K16, and W1–W17) and intercalated flow interiors (cap rocks). See **Figure 2** for well locations and major regional structural features. Histogram (left) shows the thermal neutron porosity distribution, average porosity, and standard deviation within the Grande Ronde Basalt (802 – 1,252 m depth interval, 858 data samples) from Wallula Basalt Pilot #1 well; and (right) the thermal neutron porosity distribution, average porosity, and standard deviation within the Grande Ronde Basalt (812 – 1,068 m depth interval, 714 data samples) from 100 Circles #1 well. Inset box shows average porosity (solid green line) and standard deviation (dotted red line).

The Indian Ridge Member is 79 m thick and 789 m deep at Wallula. IRM has two flows and a possible locally present flow lobe. The flows are typically medium to coarse grained, aphyric to rarely plagioclase-microphyric, and diktytaxitic (Reidel and Tolan, 2013). Two of the three key wells have penetrated the IRM, suggesting a potential pinch-out stratigraphic trap. Neutron porosity log from Wallula Basalt Pilot #1 well indicated the interflow zone (W1, W2, and W3) porosity ranges from 20.4% to 38.9%. Individual hydraulic characterization test provided a transmissivity range for the W2 injection zone of T = 0.9 to 1.8 m^2/day (k = 1,220 to 2,496 mD) (McGrail et al., 2014). The net interflow zone thickness at Wallula is 30.4 m, or 38.5% of the gross IRM thickness.

The Ortley Member contains at least 7 flows and covers ~84,000 km^2. OM flows are glassy to fine grained and aphyric (Reidel and Tolan, 2013). The OM is situated at 868 m at Wallula with a gross thickness of 187 m. Nine interflow zones (W4 to W12) were identified with a total net thickness of 58 m, or a net-to-gross ratio of 31%. Porosity ranges from 14.5% to 31.5%. Hydrologic test on W4 suggested a calculated average intrinsic permeability of 19 mD. Ortley compositions are similar to the underlying Grouse Creek member.

The Grouse Creek Member (GCM) contains at least five flows and covers most of the Columbia Basin. These flows typically lack microphenocrysts and only rarely contain plagioclase phenocrysts (Reidel and Tolan, 2013). GCM is 106 m thick and situated at 1,055.5 m below ground at Wallula. Three flows (W13, W14, and W15) were identified at Wallula with a total net thickness of 26.3 m, or a net-to-gross ratio of 24.8%. Density–neutron porosity logs indicate heterogeneous but continuous porosity throughout the interflow zones, averaging 16.9% to 29.5%.

The Wapshilla Ridge Member (WRM) has the greatest volume of all the GRB members. WRM contains at least 18 flows and is found throughout most of the Columbia Basin. These flows are glassy to fine grained, but they are abundantly plagioclase-microphyric (Reidel and Tolan, 2013). WRM is the deepest member encountered by Wallula Basalt Pilot #1 well at 1,161 m, where two interflow zones (W16 and W17) were identified. The net thickness of the interflow zones is 15.4 m, or a net-to-gross ratio of 16.8% for the 91.6 m of penetrated WRM basalt.

The flow interior interpretation from these five flow members suggested the average GRB reservoir net-to-gross ratio (fraction of total GRB thickness that meets minimum porosity and permeability, $E_{hn/hg}$) is 27%.

4.2 Pressure and temperature conditions of CO_2

Supercritical CO_2 is ideal for geologic storage due to its liquid-like density and gas-like viscosity. Supercritical CO_2 takes up less space and diffuses more easily through the pore network in reservoir rock than either gases or liquid phase CO_2, thus maximizing the storage potential

and minimizing environmental impacts. The reservoirs need to be deep enough to maintain the injected CO_2 in supercritical state (above 304.13K formation temperature and 7.3773 MPa pore pressure). The pre-injection temperature and pressure logs from Wallula Basalt Pilot #1 well suggested the CO_2 critical point was reached at 752 m bgs (**Figure 4a, b, and c**) with a density of 427.6 kg/m^3 (**Figure 4d**). Below ~800 m, the density quickly plateaued to about 640 kg/m^3. As the depth increased, the density slowly reached the maximum of 659.6 kg/m^3 at 995 m then slowly decreased (**Figure 4e**). The minimum suitable reservoir depth was set to be at 800 m bgs to buffer the topographic relief in the study area. The pressure increased along hydrostatic gradient (9.79 MPa/km), and temperature fluctuated around the average geothermal gradient of 19.36 K/km (**Figure 4b and c**). The results suggested that the density of CO_2 increased by 50% within 48 m after reaching supercritical and stayed almost constant at deeper depths. To convert calculated storage volumes to masses of CO_2 that can be stored within the GRB, we calculated the average density below 800 m to be 644 kg/m^3.

4.3 Storage for 50 MMT CO_2 and total storage resource calculation

To determine a baseline (minimum) radial plume extent for large scale CO_2, the reservoir thicknesses, formation depths, and porosities reported in **Table S2** were used to calculate the radial plume extent of 50 MMT of free phase $scCO_2$ solely occupied the pore space. Based on the modeled CO_2 plume radius of 38 meters (White et al., 2020), the resultant volume of basalt in those reservoirs, and the amount of CO_2 consumed after two years in that rock volume, we calculate that the 50 MMT of CO_2 may mineralize in 64 years. The anthropogenic carbonate minerals observed at Wallula (Battu et al., 2024; Depp et al., 2022; Lahiri et al., 2023; McGrail et al., 2017; Polites et al., 2022), aragonite ($CaCO_3$), ankerite [$Ca(Fe,Mn,Mg)(CO_3)_2$], and siderite ($FeCO_3$) are approximately twice as dense as the $scCO_2$ at reservoir conditions (644 kg/m^3, **Figure 4**), so the mineralization of CO_2 would free up 49-57% of the initial pore space occupied by the $scCO_2$, emphasizing the enhanced storage efficiency of solid phase carbonates relative to free phase or aqueous-dissolved CO_2.

Using **Eq. (2)**, the critical pressure for fluid migration into the lowest USDW Formation from the GRB reservoir is 800 kPa. The AOR for the proposed Class VI well can be defined by the 116-psi (800 kPa) isoline on the delta-pressure (Dp) map (**Figure S5**) after 30 years of injection. The Dp map for a 30-year simulation case is generated by subtracting the initial pressure from the field pressure after the 30-year CO_2 injection simulation.

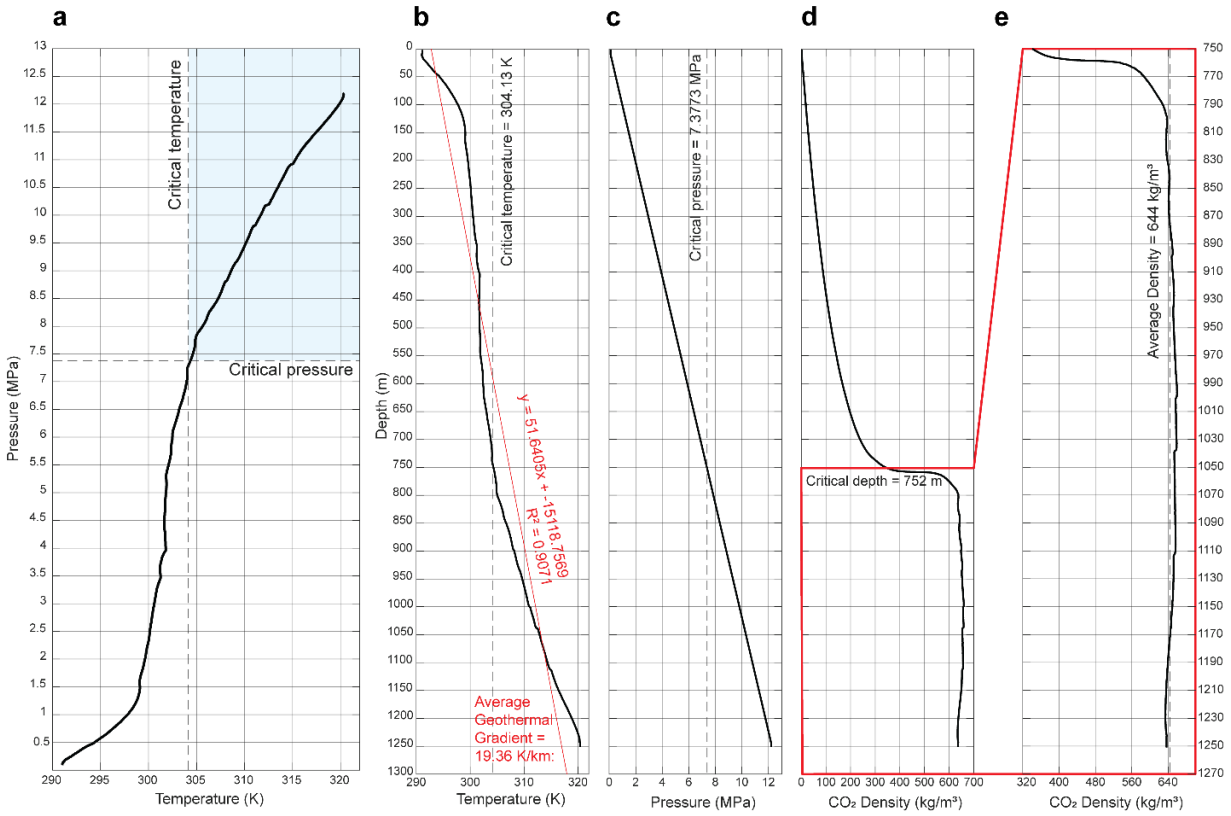

Figure 4. Carbon dioxide density analysis based on the downhole condition in the Wallula Basalt Pilot #1 well. **a.** plot of subsurface pressure versus temperature. The pressure and temperature limits (304.13 K and 7.3773 MPa) above which CO_2 is supercritical (shaded area). **b.** temperature versus depth. A geothermal gradient line is shown for a temperature gradient of 19.36 K per 1 km. **c.** plot of pressure versus depth showing normal hydrostatic pressure gradient (9.79 MPa/km). **d.** CO_2 density versus depth using pressure and temperature inputs from **Figure 4b and 4c**. Critical depth (752 m below ground) is the minimum depth for $scCO_2$. **e.** enlarged view of supercritical section of **Figure 4d** showing the variation and average $scCO_2$ density (644 kg/m^3).

As discussed in the previous section, suitable reservoir conditions for $scCO_2$ occur at >800 m below ground in the study area A_t (10,000 km^2). The gross reservoir thickness h_g is 2,200 m. The average total porosity Φ_{Total} of the interflow zones is 25.3%, and the average $scCO_2$ density ρ under reservoir condition is 644 kg/m^3.

Since the study area is on a sub-basinal scale, it is more appropriate to use the conservative values (0.2) for the geologic variable of net to total area [A_n/A_t] (IEAGHG, 2009). The net to gross thickness ratio is calculated based on petrophysical logs, where $E_{hn/hg}$ = 0.27. We approximated the effective to total porosity ratio ($E_{\Phi e/\Phi tot}$), volumetric displacement efficiency (E_v), and microscopic displacement efficiency (E_d) to the ratio for sandstone anticlinal reservoir deposited in alluvial fan environment (IEAGHG, 2009).

Using the US-DOE methodology (Goodman et al., 2011) to estimate the GRB carbon storage resource in an open

system, the calculated volumetric results (G_{CO2}) for low, medium, and high probability of storage resource potential are 40, 35, and 21 billion metric tons for P90, P50, and P10, respectively. There has been no indication so far suggesting the permeability or injectivity decreases over time as carbon mineralization occurs in basaltic reservoirs, as demonstrated by Carbfix and Carbfix2 (Clark et al., 2020; Snæbjörnsdóttir et al., 2020). For decadal timescales pertinent to commercial-scale storage of CO_2 (50 MMT over 30 years), reactive transport simulations of CO_2 fate and transport will be key for predicting time-dependent permeability changes (Liu et al., 2019; Snæbjörnsdóttir et al., 2018).

4.5 Implications for commercialization

The carbon storage feasibility assessment will accelerate scale-up and deployment of commercial CO_2 capture and storage (CCS) projects in basaltic rocks - the largest potential CO_2 storage resource in the PNW. Although this region has a strong renewable power portfolio, natural gas plants will remain essential to the PNW's energy flexibility and grid reliability for the foreseeable future, making geologic CO_2 storage a critical resource for achieving regional carbon reduction targets through 2050. The U.S. Environmental Protection Agency reported total greenhouse gas emission from point sources in Washington, Oregon, and Idaho in 2022 amount to 34.7 million metric tons. If the basalt mineralization storage resource (40 billion metric tons) in the study area can be fully leveraged, it will provide more than 1,000 years of storage capacity at the current emission level for all point sources in the PNW (**Figure S6**). The region's large renewable energy resource is attracting significant interest from developers focused on net-negative emissions technologies like direct air capture (DACCS) and bioenergy (BECCS). The carbon-negative cleantech industry could blossom here in the PNW, if we can derisk the enormous mineralization storage resource for regulators, investors and the local communities who could one day host basalt-based projects here and around the world.

The commercial-scale CO_2 storage potential of sedimentary rocks had been proven by intensive research and field deployment over the past 20 years. The PNW's CO_2 emission sources are located far from high-capacity sedimentary storage resources, which risks leaving these facilities stranded without suitable storage options. In the PNW region and around the world, basalt formations represent one of the most attractive alternative geologic storage options due to their potential for rapid mineralization of CO_2, widespread geographic distribution, and potentially large storage potential (Blondes et al., 2019; McGrail et al., 2006). However, significant work remains to support selection and development of the storage complexes to serve commercial-scale demand from the existing and potential CO_2 sources in this growing industrial area - including proven best practices for sustained, large-scale injection; technologies for characterization and monitoring to

identify and mitigate leakage and geomechanical risks; and the range of per-ton costs.

Future work will build upon knowledge developed under existing pilot-scale field projects (e.g., Wallula Basalt Pilot Project) through a focused effort to address barriers to commercial-scale mineralization storage in basalt reservoirs, and specifically at selected sites in the PNW and beyond. CO_2 sequestration via mineralization provides viable solutions for places like the upper Midwest parts of the U.S., Japan, India, Southeast Asia, and key regions of Africa that lack thick, regionally continuous sedimentary basins suitable for conventional CO_2 storage.

Supporting Information. This material is available free of charge on the International Journal of Greenhouse Gas Control website at **https://www.sciencedirect.com/journal/international-journal-of-greenhouse-gas-control** .

- General information including stratigraphic nomenclature (Figure S1) for the study area, the general flow geomorphology (Figure S2), the Grande Ronde Basalt structural map in the study area (Figure S3), major structures in the study area (Figure S4), the simulated pressure front (Figure S5), and the current carbon dioxide point sources and transportation infrastructure map for the Pacific Northwest region (Figure S6).
- Additional subsurface data including available petrophysical well logs (Table S1), and Wallula interflow zone petrophysical properties (Table S2).

AUTHOR INFORMATION

*Corresponding Authors

Ruoshi Cao, ross.cao@pnnl.gov

Quin R.S. Miller, quin.miller@pnnl.gov

NOTES

The authors declare no competing financial interest.

ACKNOWLEDGMENTS

This study was supported by Darin Damiani (DOE HQ) and the Carbon Utilization and Storage Partnership (CUSP). We thank Jake Horner (PNNL) for valuable preliminary discussions.

REFERENCES

Bachu, S., 2007. CO_2 storage in geological media: Role, means, status and barriers to deployment. Progress in energy and combustion science 34, 254-273.

Battu, A.K., Miller, Q.R., Cao, R., Owen, A.T., Schaef, H.T., 2024. 3D Quantification of Pore Networks and Anthropogenic Carbon Mineralization in Stacked Basalt Reservoirs. Environmental Science & Technology.

Blondes, M.S., Merrill, M.D., Anderson, S.T., DeVera, C.A., 2019. Carbon dioxide mineralization feasibility in the United States, Scientific Investigations Report, Reston, VA.

Bradshaw, J., Bachu, S., Bonijoly, D., Burruss, R., Holloway, S., Christensen, N.P., Mathiassen, O.M., 2007. CO2 storage capacity estimation: issues and development of standards. International journal of greenhouse gas control 1, 62-68.

Camp, V.E., Ross, M.E., Hanson, W.E., 2003. Genesis of flood basalts and Basin and Range volcanic rocks from

Steens Mountain to the Malheur River Gorge, Oregon. Geological Society of America Bulletin 115, 105-128.

Clark, D.E., Oelkers, E.H., Gunnarsson, I., Sigfússon, B., Snæbjörnsdóttir, S.Ó., Aradóttir, E.S., Gíslason, S.R., 2020. CarbFix2: CO2 and H2S mineralization during 3.5 years of continuous injection into basaltic rocks at more than 250 °C. Geochimica et Cosmochimica Acta 279, 45-66.

Depp, C.T., Miller, Q.R.S., Crum, J.V., Horner, J.A., Schaef, H.T., 2022. Pore-scale Microenvironments Control Anthropogenic Carbon Mineralization Outcomes in Basalt. ACS Earth and Space Chemistry *In Revision*.

EPA, 2013. Geologic Sequestration of Carbon Dioxide Underground Injection Control (UIC) Program Class VI Well Area of Review Evaluation and Corrective Action Guidance.

Gierzynski, A.O., Pollyea, R.M., 2017. Three-phase CO_2 flow in a basalt fracture network. Water Resources Research 53, 8980-8998.

Goldberg, D.S., Takahashi, T., Slagle, A.L., 2008. Carbon dioxide sequestration in deep-sea basalt. Proceedings of the National Academy of Sciences 105, 9920-9925.

Goodman, A., Hakala, A., Bromhal, G., Deel, D., Rodosta, T., Frailey, S., Small, M., Allen, D., Romanov, V., Fazio, J., Huerta, N., McIntyre, D., Kutchko, B., Guthrie, G., 2011. U.S. DOE methodology for the development of geologic storage potential for carbon dioxide at the national and regional scale. Int. J. Greenhouse Gas Control 5, 952-965.

Goodman, A., Sanguinito, S., Levine, J.S., 2016. Prospective CO2 saline resource estimation methodology: Refinement of existing US-DOE-NETL methods based on data availability. International Journal of Greenhouse Gas Control 54, 242-249.

Hogenson, G.M., 1964. Geology and ground water of the Umatilla River basin, Oregon. USGPO.

IEAGHG, 2009. Development of Storage Coefficients for CO_2 Storage in Deep Saline Formations; 2009/13.

IPCC, 2005. IPCC Special Report on Carbon Dioxide Capture and Storage. Prepared by Working Group III of the Intergovernmental Panel on Climate Change, New York.

Lahiri, N., Miller, Q.R.S., Cao, R., Depp, C.T., Schaef, H.T., 2023. Facile Metal Release from Pore-Lining Phases Enables Unique Carbonate Zonation in a Basalt Carbon Mineralization Demonstration. Environmental Science & Technology 57, 11843-11851.

Li, P., Jiang, J., CHENG, J., ZHAO, M., 2023. Assessment of carbon dioxide mineralization sequestration potential of volcanic rocks in Leizhou Peninsula, Guangdong Province, China. Geological Journal of China Universities 29, 76.

Liu, D., Agarwal, R., Li, Y., Yang, S., 2019. Reactive transport modeling of mineral carbonation in unaltered and altered basalts during CO2 sequestration. International Journal of Greenhouse Gas Control 85, 109-120.

McGrail, B.P., Schaef, H.T., Glezakou, V.A., Dang, L.X., Owen, A.T., 2009a. Water reactivity in the liquid and supercritical CO_2 phase: Has half the story been neglected? Energy Procedia 1, 3415-3419.

McGrail, B.P., Schaef, H.T., Ho, A.M., Chien, Y.J., Dooley, J.J., Davidson, C.L., 2006. Potential for carbon dioxide sequestration in flood basalts. Journal of Geophysical Research: Solid Earth 111.

McGrail, B.P., Schaef, H.T., Spane, F.A., Cliff, J.B., Qafoku, O., Horner, J.A., Thompson, C.J., Owen, A.T., Sullivan, C.E., 2017. Field validation of supercritical CO_2 reactivity with basalts. Environmental Science & Technology Letters 4, 6-10.

McGrail, B.P., Spane, F.A., Amonette, J.E., Thompson, C., Brown, C.F., 2014. Injection and monitoring at the Wallula basalt pilot project. Energy Procedia 63, 2939-2948.

McGrail, B.P., Sullivan, E.C., Spane, F.A., Bacon, D.H., Hund, G., Thorne, P.D., Thompson, C.J., Reidel, S.P., Colwell, F.S., 2009b. Preliminary hydrogeologic characterization results from the Wallula Basalt Pilot Study. PNWD-4129, Battelle Pacific Northwest Division, Richland, Washington.

McGrail, B.P., Sullivan, E.C., Spane, F.A., Bacon, D.H., Hund, G., Thorne, P.D., Thompson, C.J., Reidel, S.P., Colwell, F.S., 2009c. Preliminary Hydrogeologic Characterization Results from the Wallula Basalt Pilot Study. Battelle Pacific Northwest Division, Richland, Washington.

Polites, E.G., Schaef, H.T., Horner, J.A., Owen, A.T., Holliman, J.E., McGrail, B.P., Miller, Q.R.S., 2022. Exotic Carbonate Mineralization Recovered from a Deep Basalt Carbon Storage Demonstration. Environmental Science & Technology.

Reidel, S., Fecht, K., Hutter, I., Tolan, T., Chamness, M., 2020. The Olympic-Wallowa lineament: A new look at an old controversy. GSA Bulletin 133, 115-133.

Reidel, S.P., Camp, V.E., Tolan, T., Martin, B.S., 2013. The Columbia River Flood Basalt Province: Stratigraphy, Areal Extent, Volume, and Physical Volcanology. geological society of America special paper 497, 1-43.

Reidel, S.P., Martin, B.S., Petcovic, H.L., 2003. The Columbia River flood basalts and the Yakima fold belt. Field Guides 4, 87-105.

Reidel, S.P., Spane, F.A., Johnson, V.G., 2002. Natural gas storage in basalt aquifers of the Columbia basin, Pacific Northwest USA: A guide to site characterization. Pacific Northwest National Lab.(PNNL), Richland, WA (United States).

Reidel, S.P., Spane, F.A., Johnson, V.G., 2005. Potential for natural gas storage in deep basalt formations at Canoe Ridge, Washington State: a hydrogeologic assessment. Pacific Northwest National Lab.(PNNL), Richland, WA (United States).

Reidel, S.P., Tolan, T.L., 2013. The Grande Ronde Basalt, Columbia River Basalt Group. Geological Society of America Special Papers 497, 117-153.

Reidel, S.P., Tolan, T.L., Hooper, P.R., Beeson, M.H., Fecht, K.R., Bentley, R.D., Anderson, J.L., 1989. The Grande Ronde Basalt, Columbia River Basalt Group; Stratigraphic descriptions and correlations in Washington, Oregon, and Idaho. Volcanism and tectonism in the Columbia River flood-basalt province: Geological Society of America Special Paper 239, 21-53.

Sanguinito, S., Hanson, A.G., Haeri, F., Myshakin, E., Moore, J.E., Crandall, D., 2022. CO_2 Storage prospeCtive Resource Estimation Excel aNalysis (CO2-SCREEN) User's Manual: Python_V4. 1. National Energy Technology Laboratory (NETL), Pittsburgh, PA, Morgantown, WV ….

Schaef, H.T., Horner, J.A., Owen, A.T., Thompson, C.J., Loring, J.S., McGrail, B.P., 2014. Mineralization of Basalts in the CO_2-H_2O-SO_2-O_2 System. Environ. Sci. Technol. 48, 5298-5305.

Schaef, H.T., McGrail, B.P., 2009. Dissolution of Columbia River Basalt under mildly acidic conditions as a function of temperature: Experimental results relevant to the geological sequestration of carbon dioxide. Applied Geochemistry 24, 980-987.

Schaef, H.T., McGrail, B.P., Owen, A.T., 2010. Carbonate mineralization of volcanic province basalts. Int. J. Greenhouse Gas Control 4, 249-261.

Schaef, H.T., McGrail, B.P., Owen, A.T., 2011. Basalt reactivity variability with reservoir depth in supercritical CO_2 and aqueous phases. Energy Procedia 4, 4977-4984.

Snæbjörnsdóttir, S.Ó., Gislason, S.R., Galeczka, I.M., Oelkers, E.H., 2018. Reaction path modelling of in-situ mineralisation of CO2 at the CarbFix site at Hellisheidi, SW-Iceland. Geochimica et Cosmochimica Acta 220, 348-366.

Snæbjörnsdóttir, S.Ó., Sigfússon, B., Marieni, C., Goldberg, D., Gislason, S.R., Oelkers, E.H., 2020. Carbon dioxide storage through mineral carbonation. Nature Reviews Earth & Environment 1, 90-102.

Snæbjörnsdóttir, S.Ó., Wiese, F., Fridriksson, T., Ármansson, H., Einarsson, G.M., Gislason, S.R., 2014. CO2 storage potential of basaltic rocks in Iceland and the oceanic ridges. Energy Procedia 63, 4585-4600.

Span, R., Wagner, W., 1996. A new equation of state for carbon dioxide covering the fluid region from the triple-point temperature to 1100 K at pressures up to 800 MPa. Journal of physical and chemical reference data 25, 1509-1596.

Stanfield, C.H., Miller, Q.R.S., Battu, A.K., Lahiri, N., Nagurney, A.B., Cao, R., Nienhuis, E.T., DePaolo, D.J., Latta, D.E., Schaef, H.T., 2024. Carbon Mineralization and Critical Mineral Resource Evaluation Pathways for Mafic–Ultramafic Assets. ACS Earth and Space Chemistry.

Strait, S.R., Mercer, R.B., 1987. Hydraulic Property Data from Selected Test Zones on the Hanford Site. Rockwell International.

Sullivan, E.C., Hardage, B.A., McGrail, B.P., Davis, K.N., 2011. Breakthroughs in seismic and borehole characterization of basalt sequestration targets. Energy Procedia 4, 5615-5622.

Swanson, D.A., Tl, W., Pr, H., Rd, B., 1979. Revisions in stratigraphic nomenclature of the Columbia River Basalt Group. U.S. Geological Survey, Washington, D.C.

Vishal, V., Verma, Y., Chandra, D., Ashok, D., 2021. A systematic capacity assessment and classification of geologic CO2 storage systems in India. International Journal of Greenhouse Gas Control 111, 103458.

Weise, F., Fridriksson, T., Ármannsson, H., 2008. CO2 fixation by calcite in high-temperature geothermal systems in Iceland.

White, S.K., Spane, F.A., Schaef, H.T., Miller, Q.R., White, M.D., Horner, J.A., McGrail, B.P., 2020. Quantification of CO_2 mineralization at the Wallula basalt pilot project. Environmental Science & Technology 54, 14609-14616.

Xiong, W., Wells, R.K., Horner, J.A., Schaef, H.T., Skemer, P.A., Giammar, D.E., 2018. CO_2 Mineral Sequestration in Naturally Porous Basalt. Environmental Science & Technology Letters 5, 142-147.

880